SAND2014-20118R

Compact Neutron HBT Model Notes and Comments

Eric Keiter *

November 20, 2014

Sandia National Laboratories is a multi-program laboratory managed and operated by Sandia Corporation, a wholly owned subsidiary of Lockheed Martin Corporation, for the U.S. Department of Energy's National Nuclear Security Administration under contract DE-AC04-94AL85000.

1 Introduction

This writeup is intended to address some questions about the compact model for neutron effects in HBT's that came up during the QASPR independent review. A detailed description of the model is given in the Sandia Models reference guide [1]. A good description of an early version of the model is given in the FY11 Milestone report [2].

- explain why compact neutron model cannot use the XPD(TCAD) HBT neutron model μ table.
- explain why compact neutron model is not a modification of the VBIC [9], Spice Gummel-Poon (SGP) [8] , or FBH [10]) model recombination term.
- Describe addition of thermal annealing to compact model, and preliminary results.

This writeup includes a very simplified development of a neutron model in sections 2, 3 and 4. In the actual Xyce neutron HBT model, the carrier densities are computed with a detailed analytical model. In the model presented in this writeup, the carrier approximations have been greatly simplified, and this leads to an expression very similar to that of standard bipolar compact models. Despite the simplification, this model has just enough complexity to explain why the Xyce and XPD models should require a different μ table, and this is explained in section 5. Note that parts of this writeup were originally developed to explain the differences between an early version of the compact neutron model (level=222) and a more recent version (level=333), but the arguments should largely apply to comparisons to XPD as well.

The presentation of this simplified model poses the question, "why not simply use this model?", or, relatedly, "why not simply modify the recombination terms of an existing bipolar model?". There are various reasons why this simplified approach is not likely to be sufficient, and a few of these are explained in section 6.

Finally, there is interest in adapting the compact model to include thermal annealing. Preliminary work will be described for this in section 7.

*author is with Sandia National Laboratories, P.O. Box 5800, Albuquerque, NM 87185. (e-mail: erkeite@sandia.gov)

2 Recombination

In the neutron model, the recombination calculation is based on a modified SRH [6] expression that approximates the statistics of trap-assisted recombination:

$$R(x,t) = \sigma v_{th} N_{FP} \mu(v,t) \frac{np - (np)_0}{n + p + 2\sqrt{(np)_0}} \tag{1}$$

In equation 1, N_{FP} is the Frenkel-Pair defect density, σ is the carrier capture cross section, and v_{th} is the thermal velocity of carriers. n and p are the electron and hole densities, respectively, computed in the carrier model. $(np)_0$ is the asymptotic value of their product, and is similar to the more familiar n_i^2. t is the time elapsed since the radiation pulse. Note that as there is a lack of detailed defect data for III-V materials, the equation 1 assumes a single defect in the center of the bandgap. So this is related to the more conventional SRH expression for trap-assisted tunnelting as:

$$R = \frac{pn - n_i^2}{\tau_n \left[p + n_i exp\left(\frac{E_i - E_t}{kT}\right)\right] + \tau_p \left[n + n_i exp\left(\frac{E_t - E_i}{kT}\right)\right]} \tag{2}$$

$$= \frac{N_t v_{th} \sigma_n \sigma_p pn - n_i^2}{\sigma_p \left[p + n_i exp\left(\frac{E_i - E_t}{kT}\right)\right] + \sigma_n \left[n + n_i exp\left(\frac{E_t - E_i}{kT}\right)\right]} \tag{3}$$

$$= N_t v_{th} \sigma \frac{pn - n_i^2}{[p + n_i] + [n + n_i]} \tag{4}$$

$$= N_t v_{th} \sigma \frac{pn - n_i^2}{p + n + 2n_i} \tag{5}$$

$$= N_t v_{th} \sigma \frac{pn - (np)_0}{p + n + 2\sqrt{(np)_0}} \tag{6}$$

Equation 6 was derived by assuming that the trap energy E_t is in the center of the bandgap, thus equal to E_i, and that the collision cross section for electrons and holes is equal, or $\sigma_n = \sigma_p$. Finally, n_i^2 is replaced by $(np)_0$. The main difference between equation 1 and equation 6 is the empirical variable μ, which is an dimensionless empirical fitting parameter. It contains the time evolution (i.e. annealing) of R, and also contains the dependence of the annealing rate on bias. Equation 1 is fitted to radiation test data for a device at a particular current density and time through the parameter $\mu(v,t)$.

2.1 Numerical Spatial Integrals

Equation 1 provides a recombination rate as a function of location in the device. In the model, it is necessary to convert the one-dimensionally spatially dependent rates ($R(x,t)$) into terminal currents. This is accomplished by numerically evaluating one-dimensional integrals, given by:

$$I_{be}(t) = qA_{be} \int_{x_e}^{x_b} R(x,t)dx \tag{7}$$

$$I_{bc}(t) = qA_{bc} \int_{x_b}^{x_c} R(x,t)dx \tag{8}$$

A_{be} and A_{bc} are the cross-sectional areas for the base-emitter and base-collector, respectively. q is unit charge. x_e, x_b, and x_c are the locations of the emitter, base, and collector contacts. These integrals are evaluated using trapezoid rule integration.

3 Simple closed-form expression for I_{be}

A very simple approximation can be used to get a closed form for I_{be}, rather than relying on the spatial integrals in equation 8. In most HBT devices, the recombination from the base will dominate I_{be}, and so any terms from outside the base can be excluded. Furthermore, the doping profile in every region is flat, meaning that the majority density is constant. Finally, in Npn devices, the base minority carrier (electrons) will be subject to a very high electric field and will be at a constant saturation velocity. This means that the minority carrier can be assumed to be constant with depth as well. This gives:

$$I_{be}(t) = qA_{be}\int_{x_e}^{x_b} R(x,t)dx \tag{9}$$

$$= qA_{be}W_{base}R(t) \tag{10}$$

$$= qA_{be}W_{base}\left[\sigma v_{th}N_{FP}\mu(v,t)\frac{np-(np)_0}{n+p+2\sqrt{(np)_0}}\right] \tag{11}$$

$$= A_{be}\mu(v,t)P\left[\frac{np-(np)_0}{n+p+2\sqrt{(np)_0}}\right] \tag{12}$$

where:

$$P = qW_{base}\sigma v_{th}N_{FP} \tag{13}$$

For the sake of simplicity, in this discussion n_i^2 is used instead of $(np)_0$, giving:

$$I_{be}(t) = A_{be}\mu(v,t)P\left[\frac{np-n_i^2}{n+p+2n_i}\right] \tag{14}$$

Note that A_{be} is the junction area parameter used by the compact model, and μ is the normalized empirical factor.

4 Solving the closed form expression

The closed form equation 12 needs values of n and p, as well as q, A_{be}, W_{base}, σ, v_{th}, N_{FP}, μ and n_i. Parameter values for this example are given in table 1, which are for a P-type GaAs base region. In an Npn device, the base value for p will simply be equal to N_A. The base value for n can be approximated using the so-called "law of the junction". The law of the junction is based on the equilibrium relationship between the electron and hole densities (n and p) and the intrinsic concentration. This is given by:

$$np = n_i^2 \tag{15}$$

This approximation applied to the equilibrium case, meaning a diode that is unbiased. If the diode is biased, then the expression needs to be modified, and is then given by:

$$p = n_i^2 e^{(E_i - F_P)/kT} \tag{16}$$

$$n = n_i^2 e^{(F_N - E_i)/kT} \tag{17}$$

$$pn = n_i^2 e^{(F_N - F_P)/kT} \tag{18}$$

$$pn = n_i^2 e^{qV_A/kT} \tag{19}$$

Which gives for electrons:

$$n = \frac{n_i^2}{p}e^{qV_A/kT} = \frac{n_i^2}{N_A}e^{qV_A/kT} \tag{20}$$

Parameter	Value
N_A	1.0e+19
N_D	0.0
q	1.602e-19
Abe (junction area)	6.25e-6
W_{base}	3.0e-6
σ	1.5e-13
v_{th}	1.0e+7
N_{FP}	2.9467e+16
P	2.12428e-14
$\sqrt{(np)_0} \approx n_i$	1.79e+6
n_i^2/N_A	3.2041e-07

Table 1: Table of parameters for the Npn device.

This can be substituted into equation 14, giving:

$$I_{be}(t) = A_{be}\mu(v,t)P\left[\frac{\left(\frac{n_i^2}{N_A}e^{qV_A/kT}\right)N_A - n_i^2}{\left(\frac{n_i^2}{N_A}e^{qV_A/kT}\right) + N_A + 2n_i}\right] \tag{21}$$

For a P-type base, electrons will have a much lower density than the majority carrier, holes. For example, using the given parameters, the value of n for an applied bias of $V_A = 1.3$ is around $1.0e+15$, or four orders of magnitude lower than N_A. That means that equation 21 can be simplified further, to:

$$I_{be}(t) = A_{be}\mu(v,t)P\left[\frac{n_i^2}{N_A + 2n_i}\right]\left[e^{qV_A/kT} - 1\right] \tag{22}$$

This is, of course, very closely related to the standard diode equation. This is not very surprising given that this derivation largely followed the same derivation of the recombination diodes used in the Gummel-Poon(SGP). See, for example, the derivation in Shur [7]. Typically, to account for non-idealities, it is standard to add a non-ideality factor, α giving:

$$I_{be}(t) = A_{be}\mu(v,t)P\left[\frac{n_i^2}{N_A + 2n_i}\right]\left[e^{\frac{qV_A}{\alpha kT}} - 1\right] \tag{23}$$

5 Putting it together, comparing differences

Both the level=222 device and the level=333 device use equations similar to equation 23, but with slightly different details. Primarily, between the two models, the handling of carrier discontinuities at the heterojunction was changed. (hopefully for the better). As a simple experiment, assuming a constant $\mu = 1.0$, is to make the minority carrier density have a consistent offset. For this experiment, the density offset chosen is $C = 1.0e+12$, so substituting into equation 21:

$$I_{be}(t) = A_{be}\mu(v,t)P\left[\frac{\left(C + \frac{n_i^2}{N_A}e^{\frac{qV_A}{\alpha kT}}\right)N_A - n_i^2}{\left(C + \frac{n_i^2}{N_A}e^{\frac{qV_A}{\alpha kT}}\right) + N_A + 2n_i}\right] = A_{be}\mu(v,t)P\left[\frac{\left(C + \frac{n_i^2}{N_A}e^{\frac{qV_A}{\alpha kT}}\right)N_A - n_i^2}{N_A + 2n_i}\right] \tag{24}$$

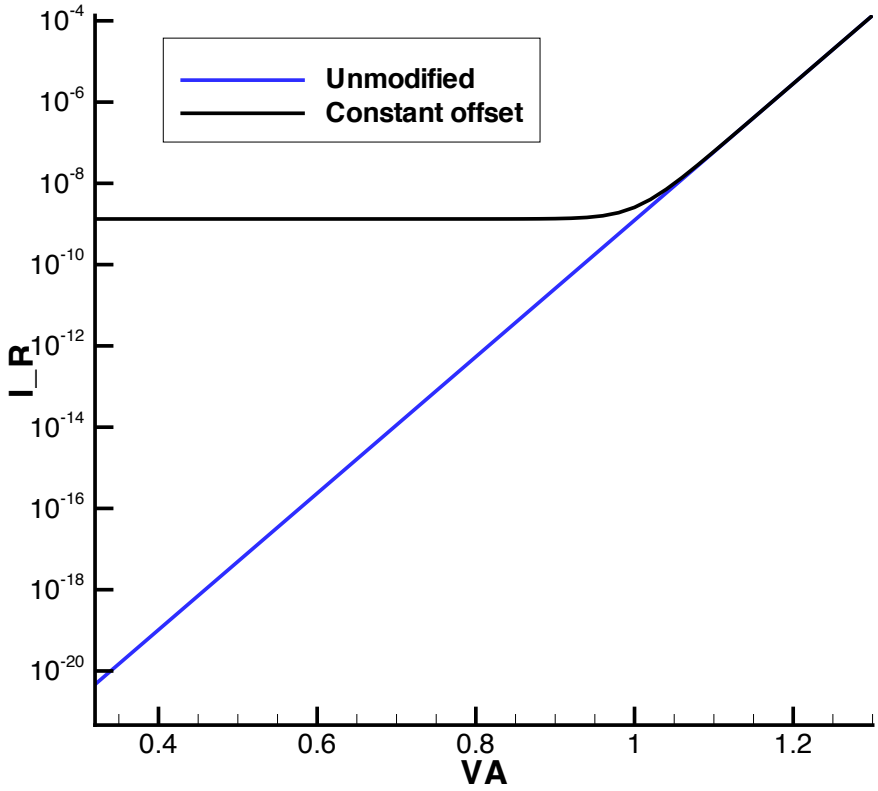

Figure 1: Recombination vs. applied voltage, for $C = 0.0$(unmodified) and $C = 1.0 + 12$ (constant offset).

Figure 1 shows the effect of adding a constant offset to the electron concentration. Equation 24 is plotted for both $C = 0.0$ and $C = 1.0e + 12$. At low bias (where the minority carrier density is really low) this has a really big impact on the computed recombination rate. At high bias (above 1 volt), where the computed minority carrier density is much higher than the offset, it doesn't have much impact. This probably explains why the level=222 and level=333 match well at high bias and match poorly at low bias. The same argument applies for comparisons to XPD.

6 Comments on Simplified Model

The model presented in the previous sections suggests that one could develop a neutron model using this simplified approach. There are several reasons why this could be problematic.

6.1 Lack of V_{be} dependence in I_{bc} diode

- The VBIC [9], Gummel-Poon(SGP) [8], FBH [10] and other bipolar compact models treat recombination using a diode term similar to equation 22.
- In the SGP, VBIC, and FBH models, these recombination diodes are applied at the base-emitter and base-collector. And, they are completely independent of each other. The I_{be} recombination diode is only dependent on V_{be} bias, and the I_{bc} diode is only dependent on the V_{bc} bias. This may be sufficient for normal environment operation, but is not for our problem.
- The reason this can't work for the neutron problem is that the base-collector carrier density has a strong dependence on V_{be}, which can be observed in figure 2. In the figure, each color represents a different V_{bc} value, and the different curves within each color represent a range of V_{be} values.

6.2 Handling of μ table

To handle $\mu(v,t)$ properly, it is necessary to be able to do complex multi-dimensional spline interpolations. The VBIC [9] and FBH [10] models are developed in Verilog-A, and imported into Xyce using a model compiler. The verilog-A language doesn't have a convenient way to implement these spline interpolations.

6.3 Choice of Bipolar Compact Model

Early in the project both the VBIC [9] and FBH [10] models were under consideration. Modifying the VBIC directly would have added an additional risk to the project, if the analysts later were to decide to use the FBH instead.

For similar reasons, Xyce radiation models have historically been developed outside the original normal environment models. Another use case: Years ago, we implemented a photocurrent model in the Berkeley BSIMSOI version 2. A year later, Berkeley released version 3, and all that work had to be re-done in the new version. Instead of doing this, we chose to implement radiation models in completely separate modules, that can then be applied in parallel to the normal environment model of choice. For practical reasons, this has been the modeling approach used for all subsequent work.

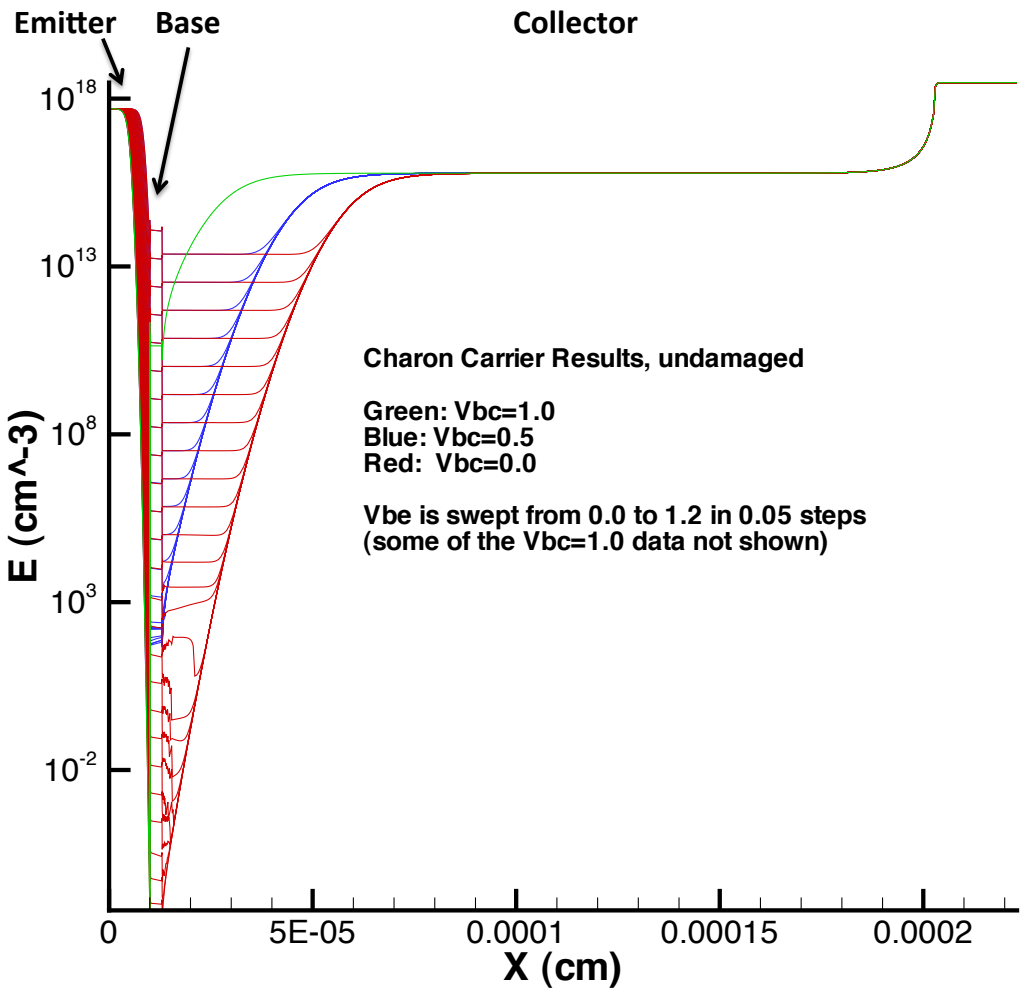

Figure 2: TCAD (Charon) result, electrons

7 Preliminary work on Thermal Annealing

Thermal annealing is of interest, due to the fact that in testing parts are often exposed to neutrons while "off" and then turned on later (sometimes much later) for purposes of measuring annealing curves. During the "off" period the device may undergo a small amount of thermal annealing. The consequence of this is that the early time portion of the annealing curve will have a shallower slope.

Thermal annealing in the empirical neutron model can be modeled by adding a zero current (or zero bias) entry in the μ table, which includes a small amount of annealing. A set of preliminary calculations using this approach is shown in figure 3.

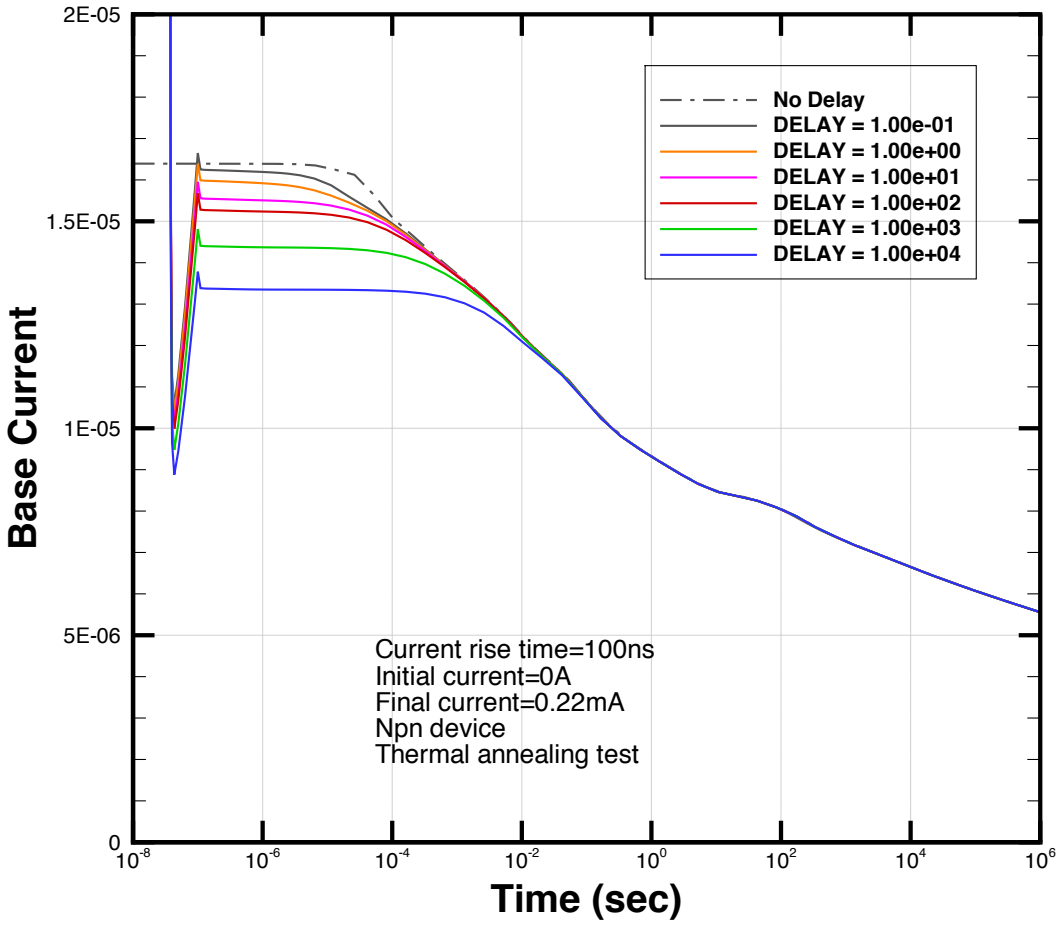

Figure 3: Preliminary Thermal annealing result

References

[1] Eric R. Keiter, Tom V. Russo, Richard L. Schiek, Jason C. Verley, and Erik C. Zeek Xyce Parallel Electronic Simulator: Reference Guide, Version 6.2. Technical Report SAND2014-18939, Sandia National Laboratories, Albuquerque, NM, September 2014.

[2] Eric R. Keiter et al. Progress report for simulation of III-V HBTs under transient neutron irradiation: QASPR/ASC Level II Milestone # 3963. Technical Report SAND2012-4240, Sandia National Laboratories, Albuquerque, NM, May 2012.

[3] Matthias Rudolph, *Introduction to Modeling HBT's*, Artech House, Norwood, MA, 2006.

[4] Ben Streetman and Sanjay Banerjee, *Solid State Electronic Devices*, Prentice Hall, 5th edition, 1999.

[5] William Liu, *Fundamentals of III-V Devices: HBTs, MESFETs, and HFETs/HEMTs*, Wiley-Interscience, New York, 1999.

[6] W. Shockley and W. T. Read. *Statistics of the recombinations of holes and electrons* Phys. Rev., 87:835–842, Sep 1952.

[7] M. Shur. *Physics of Semiconductor Devices*. Prentice Hall, 1990.

[8] H. K. Gummel and H. C. Poon. An integral charge control model of bipolar transistors. *Bell Sys. Techn. J.*, May-June:827–852, 1970.

[9] Colin McAndrew, Mark Dunn, Shahriar Moinian, and Michael Schröter. VBIC95, The Vertical Bipolar Inter-Company Model. *IEEE Journal of Solid-State Circuits*, 31(10):1476–1483, 1996.

[10] Matthias Rudolph. Documentation of the fbh hbt model, 2005.